engineering proceedings

MDPI

Proceeding Paper

Mathematical Models of Systems for Measuring Pressure of Gas–Liquid Media and Their Comparative Analysis †

Petr Velmisov * and Andrey Ankilov

Department of Higher Mathematics, Ulyanovsk State Technical University, 432027 Ulyanovsk, Russia; ankil@ulstu.ru

* Correspondence: velmisov@ulstu.ru

† Presented at the 15th International Scientific Conference TechSys 2026—Engineering, Technologies and Systems, Plovdiv, Bulgaria, 14–16 May 2026.

Abstract

The paper considers a linear differential operator and a nonlinear integro-differential operator, on the basis of which the equations of vibration of a deformable plate are written down. The nonlinear operator takes into account the nonlinearity of the longitudinal force arising from the elongation of the plate due to its deformation. Based on the proposed equations, the mathematical models of the mechanical system "pipeline–pressure sensor" are developed. The system consists of a pipeline attached at one end to the combustion chamber of an aircraft engine and a sensor designed to measure the pressure in the combustion chamber at the other end. The sensing element of the sensor that transmits the pressure information is a deformable plate. The models take into account the transfer of heat flow through the pipeline with the working medium (gas or liquid) from the engine to the elastic element and the aerohydrodynamic effect of this medium on the plate. On the basis of the small parameter method, the asymptotic equations describing the joint dynamics of the working medium in the pipeline and the deformable element of the sensor are obtained. The dynamics study is based on the application of the Galerkin method and numerical experiment in Mathematica 12.0. The case of rigid fixation of the elastic element ends is considered. A comparative analysis of solutions for linear and nonlinear models is made. The insignificant influence of the nonlinearity of the longitudinal force on the value of the plate deflection is shown.

Keywords: aerohydroelasticity; pressure sensor; elastic plate; nonlinear differential operator; dynamics; Galerkin method

Check for updates

Academic Editors: Nikola G. Shakev, Valyo N. Nikolov, Nikolay R. Kakanakov and Sevil A. Ahmed-Shieva

Published: 11 August 2026

Copyright: © 2026 by the authors. Licensee MDPI, Basel, Switzerland. This article is an open access article distributed under the terms and conditions of the Creative Commons Attribution (CC BY) license.

1. Introduction

The study of the dynamics and stability of deformable elements is of great importance in the design and operation of structures, devices, and plants for various purposes that interact with the flow of gas or liquid [1–21]. In some cases, the impact of the flow can lead to amplitudes, frequencies and velocities of oscillations of elastic elements that do not allow for the reliable operation of systems and do not ensure the functional accuracy of their work. Such a problem arises in the design of pressure sensors. Many works are devoted to the theoretical and practical issues of pressure sensor design. Let us list some of the latest ones [15–27]. References [17–23,26,27] are devoted to descriptions of sensors of measuring systems, the principles of their operation, and their technical characteristics. Some works are devoted to describing the materials and manufacturing technologies of sensors [17,18,24].

Pressure sensors operating in aircraft and rocket engines are impacted by high temperatures and increased vibration accelerations, which are most pronounced in transient modes of engine operation. Such extreme operating conditions lead to additional measurement error and even to the destruction of the elastic-sensitive element of the sensor. One of the ways of solving this problem is ensuring the optimal design of the mechanical system "pipeline–pressure sensor". In this system, the sensor is located some distance from the engine and connected to it by means of a pipeline, which weakens the impact of temperature and vibration accelerations. Mathematical models of the system "pipeline–pressure sensor" were considered, for example, in [15,16].

This paper investigates the joint dynamics of a pressure sensor element and the working medium in a pipeline through mathematical models representing the initial boundary value problems for systems of differential equations. The study of the dynamics of the elastic element applies the Galerkin method and numerical experiments.

This paper studies the influence of the nonlinearity of the longitudinal force arising from the elongation of the pressure sensor-sensing element due to its deformation, based on a comparison of linear and nonlinear models of a solid deformable body, describing the oscillations in the sensor sensing element.

2. Asymptotic Models of Deformable Solid Bodies

In this paper, we study the dynamics of a deformable plate subjected to aerohydrodynamic and thermal effects. Let the deflection of a plate of length H and thickness h depending on the coordinate of the plate point be $y \in [0, H]$, and time $t \geq 0$ is described by the function $w(y, t)$. The case of rigid fixation of the plate ends is considered:

$$w(0, t) = w_y(0, t) = 0, w(H, t) = w_y(H, t) = 0. \quad (1)$$

Linear (2) and nonlinear (3) mathematical models of a deformable solid are proposed to describe the plate dynamics:

$$L(w(y, t)) \equiv Mw_{tt} + Dw_{yyyy} + N(t)w_{yy} + \gamma w + \beta_1 w_t + \beta_2 w_{yyyyt}; \quad (2)$$

$$J(w(y, t)) \equiv L(w(y, t)) - w_{yy}\left(\mu \int_0^H w_y^2 dy + \eta \left(\int_0^H w_y^2 dy\right)_t\right). \quad (3)$$

The indices at the bottom denote partial derivatives of the corresponding variables. In operators (2) and (3) the following notations of the mechanical characteristics of the deformed plate are introduced: M, D are the linear mass and bending stiffness of the plate; $N(t)$ is the function describing the compressive or tensile force on the plate; γ is the stiffness coefficient of the crimped layer of the plate; β_1 is the coefficient of external damping; β_2, η are the coefficients describing the internal damping of the plate; μ is the coefficient depending on the strength and geometrical characteristics of the plate. The nonlinear model (3) takes into account the nonlinearity of the longitudinal force resulting from the elongation of the plate due to its deformation.

To calculate the linear mass and bending stiffness of the plate, we use the following formulas:

$$D = \frac{Eh^3}{12(1 - \nu^2)}, \quad M = \rho_0 h, \quad (4)$$

where E is the modulus of elasticity of the plate; ν is the Poisson's ratio; ρ_0 is the density of the plate.

https://doi.org/10.3390/engproc2026150129

Taking into account the thermal effect on the plate, the variable compressive force coefficient is as follows:

$$N(t) = N_0 + \frac{E\alpha_T}{1-\nu}\int_0^h T(x,t)dx, \tag{5}$$

where N_0 is the constant component of the force created when fixing the plate; α_T is the temperature coefficient of linear expansion; $T(x,t)$ is the law of the temperature change along the thickness of the element.

As the plate deformation and the temperature coefficient of linear expansion of the plate material are small, let us represent them in the form of a small parameter $\varepsilon = \frac{h}{H}$ expansion:

$$w(y,t) = w_0(y) + \varepsilon w_1(y,t) + \dots, \quad \alpha_T = \varepsilon\alpha_{T1} + \dots \tag{6}$$

Restricting to terms of order ε, let us represent the operators $L(w(y,t)),\ J(w(y,t))$ in the following form:

$$L(w(y,t)) = L_1(w_0(y)) + \varepsilon L_2(w_0(y), w_1(y,t)), \quad J(w(y,t)) = J_1(w_0(y)) + \varepsilon J_2(w_0(y), w_1(y,t)). \tag{7}$$

Let us introduce the notation $N_1(t) = \frac{E\alpha_{T1}}{1-\nu}\int_0^h T(z,t)dz$. Then, substituting (6) into (2), (3), we obtain

– for model (2)

$$\begin{cases} L_1(w_0(y)) = Dw_{0yyyy} + N_0 w_{0yy} + \gamma w_0, \\ L_2(w_0(y), w_1(y,t)) = Mw_{1tt} + Dw_{1yyyy} \ + N_1(t)w_{0yy} + N_0 w_{1yy} + \gamma w_1 + \beta_1 w_{1t} + \beta_2 w_{1yyyyt}; \end{cases} \tag{8}$$

– for model (3)

$$\begin{cases} J_1(w_0(y)) = L_1(w_0(y)) - \mu w_{0yy}\int_0^H w_{0y}^2 dy, \\ J_2(w_0(y), w_1(y,t)) = L_2(w_0(y), w_1(y,t)) + \beta_2 w_{1yyyyt} - \\ -\mu w_{1yy}\int_0^H w_{0y}^2(y)dy - 2w_{0yy}\left(\mu\int_0^H w_{0y}(y)w_{1y}(y,t)dy + \eta\int_0^H w_{0y}(y)w_{1yt}(y,t)dy\right). \end{cases} \tag{9}$$

By virtue of the boundary conditions (1) for the function $w(y,t)$, we obtain the boundary conditions for the functions $w_0(y),\ w_1(y,t)$:

$$w_0(0) = w_{0y}(0) = 0, \quad w_0(H) = w_{0y}(H) = 0, \tag{10}$$

$$w_1(0,t) = w_{1y}(0,t) = 0, \quad w_1(H,t) = w_{1y}(H,t) = 0. \tag{11}$$

3. Mathematical Model of the Pressure Measurement System

Let the plate be an elastic element in the system for measuring the pressure of the working medium in the combustion chamber of an aircraft engine. The system is shown in Figure 1, where l is the length of the pipeline 2 connecting the pressure sensor 3 with the combustion chamber 1; $T_*(t)$ is the law of temperature change at the inlet of the pipeline (at the outlet of the combustion chamber); $T_1(x,t)$ is the law of the temperature change in the working medium along the length of the pipeline 4; $T_2(x,t)$ is the law of the temperature change along the thickness of the element; T_0 is the ambient temperature ($T_0 = const$). We consider a mathematical model of heat flow transmission through a pipeline with a working medium (gas or liquid) from an aircraft engine to a sensor measuring the pressure of this medium. At one end ($x = -l$) of the pipeline, fixed at the outlet of the engine combustion chamber, there is a change in the pressure of the working medium. At the other

end ($x \in [0, h]$) of the pipeline, there is a sensor designed to measure this pressure, the working element of which is an elastic plate 5 The velocity field of the working medium is assumed to be flat.

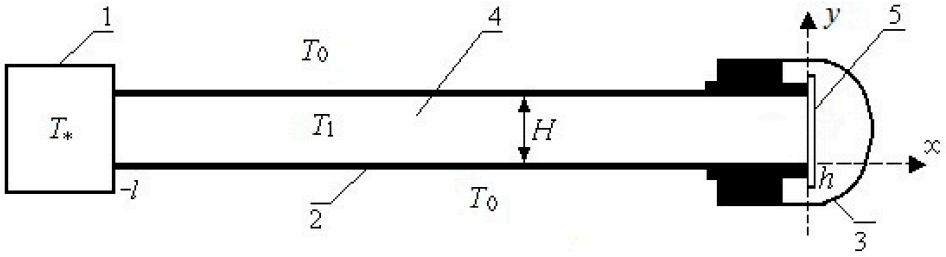

Figure 1. Pipe with sensor.

Let us introduce notations: $\Phi(x, y, t)$ is the velocity potential of the gas–liquid medium; $P(x, y, t)$ is the pressure in this medium; $g(x, y, t) = 0$ is the equation of the elastic element surface; $F(y, t)$ is the law of the change in the working medium pressure at the combustion chamber outlet (at the pipeline inlet). Then, the mathematical formulation of the problem in the incompressible medium model is as follows:

$$\Phi_{xx} + \Phi_{yy} = 0, \qquad x \in (-l, 0), \ y \in (0, H), \tag{12}$$

$$\Phi_x g_x + \Phi_y g_y = -g_t, \qquad g(x, y, t) = 0, \quad y \in (0, H), \tag{13}$$

$$L(w(y, t)) = P - \overline{P}, \quad y \in (0, H), \tag{14}$$

$$P = P_0 - \rho\left(\Phi_t + \frac{1}{2}\Phi_x^2 + \frac{1}{2}\Phi_y^2\right), \tag{15}$$

$$P(-l, y, t) = F(y, t), \quad y \in (0, H), \tag{16}$$

$$\rho c_1 T_{1t} = k_1 T_{1xx} - \beta(T_1 - T_0), \ x \in (-l, 0), \tag{17}$$

$$T_1(-l, t) = T_*(t), \tag{18}$$

$$T_{1x}(0, t) = 0, \tag{19}$$

$$\rho_0 c_2 T_{2t} = k_2 T_{2xx}, \ x \in (0, h), \tag{20}$$

$$T_{2x}(h, t) = 0, \tag{21}$$

$$-k_2 T_{2x}(0, t) = \alpha\,(T_1 - T_2)|_{x=0}. \tag{22}$$

Here, P_0 is the pressure in the resting liquid; $\overline{P}$ is the external pressure on the plate; ρ is the density of the medium; ρ_0 is the density of the plate material; k_1, k_2 are the heat conductivity coefficients of the medium and the plate material, respectively; c_1, c_2 are the heat capacity coefficients of the medium and the plate; β is the heat exchange coefficient between the pipeline surface and the environment; α is the heat exchange coefficient between the working medium and the plate.

Laplace Equation (12) describes the motion of incompressible medium in the pipeline; boundary condition (13) defines the law of non-flow of gas–liquid medium through the surface of the element; Equation (14) describes the dynamics of the elastic element; pressure in the working medium (15) is determined by the Lagrange–Cauchy integral; Equation (16) defines the law of equality of pressures at the inlet to the pipeline and at the outlet from the combustion chamber of the engine; Equations (17) and (20) describe the law of temperature distribution along the length of the pipeline and along the thickness of the plate, respectively; Equation (18) defines the law of temperature change at the engine outlet;

Equation (19) means that the heat flux penetrating through the left boundary of the plate $x = 0$ is negligibly small, due to the smallness of the plate thickness and the presence of a vacuum to the right of it; (21) is the thermal insulation of the outer side of the plate, to the right of which there is a vacuum; (22) is the condition of heat exchange between the plate and the working medium in the sensor cavity.

Considering (6), let us write the surface equation of the elastic element in the form

$$g(x, y, t) = x - w(y, t) = x - w_0(y) - \varepsilon w_1(y, t) - \ldots = 0. \tag{23}$$

Let us represent the functions $\Phi(x, y, t)$, $F(y, t)$ in the form of a small-parameter ε expansion:

$$\Phi(x, y, t) = \varepsilon\varphi(x, y, t) + \ldots, \qquad F(y, t) = P_0 + \varepsilon P_*(y, t) + \ldots . \tag{24}$$

where $P_*(y, t)$ is the overpressure at the pipeline inlet (in section $x = -l$).

Substituting (23), (24) into Equations (12)–(16) and restricting ourselves to terms of order ε, we obtain an asymptotic model of the problem in the first approximation:

$$\varphi_{xx} + \varphi_{yy} = 0, \quad x \in (-l, 0), \ y \in (0, H), \tag{25}$$

$$\varphi_x(w_0(y), y, t) - w_{0y}(y)\varphi_y(w_0(y), y, t) = w_{1t}(y, t), \ y \in (0, H), \tag{26}$$

$$W_1(w_0(y)) = P_0 - \overline{P}, \quad y \in (0, H), \tag{27}$$

$$W_2(w_0(y), w_1(y, t)) = -\rho\varphi_t(w_0(y), y, t), \ y \in (0, H), \tag{28}$$

$$-\rho\varphi_t(-l, y, t) = P_*(y, t), \quad y \in (0, H). \tag{29}$$

Here, $W_1(w_0(y))$, $W_2(w_0(y), w_1(y, t))$ is understood as $L_1(w_0(y))$, $L_2(w_0(y), w_1(y, t))$ for model (2) and $J_1(w_0(y))$, $J_2(w_0(y), w_1(y, t))$ for model (3).

4. Solving the Problem in the Zero Approximation

Equation (27) is an ordinary differential or integro-differential equation for one unknown function $w_0(y)$ with boundary conditions (10). From (27), we obtain:

– For model (2)

$$Dw_{0yyyy} + N_0 w_{0yy} + \gamma w_0 = P_0 - \overline{P}; \tag{30}$$

– For model (3)

$$Dw_{0yyyy} + N_0 w_{0yy} + \gamma w_0 - \mu w_{0yy} \int_0^H w_{0y}^2 dy = P_0 - \overline{P}. \tag{31}$$

If the difference between the resting pressure and the external load distributed over the plate is $P_0 - \overline{P} = 0$, then for each model we obtain $w_0(y) \equiv 0$.

Let us take a non-zero difference $P_0 - \overline{P} = 2 \cdot 10^4$. Assume that the plate thickness $h = 7 \cdot 10^{-4}$ and length $H = 2 \cdot 10^{-2}$ is made of aluminium; then, density $\rho_0 = 2700$, modulus of elasticity $E = 7 \cdot 10^{10}$, and Poisson's ratio $\eta = 0.34$. According to (4), $D = 2.262$, $M = 1.89$. Assume that the constant component of the force is $N_0 = 10^5$, stiffness coefficient of the crimping layer of the plate is $\gamma = 4$, and coefficients at nonlinear terms are $\mu = 30$, $\eta = 20$. All values are given in SI. In Mathematica 12.0, we numerically find solutions to the boundary value problems in Equations (30) and (31) with boundary conditions (10). The solution of Equation (30) is shown in Figure 2. Figure 3 shows the

https://doi.org/10.3390/engproc2026150129

difference between the solutions of Equations (30) and (31), where $w_{01}(y), w_{02}(y)$ are the solutions of Equations (30) and (31), respectively.

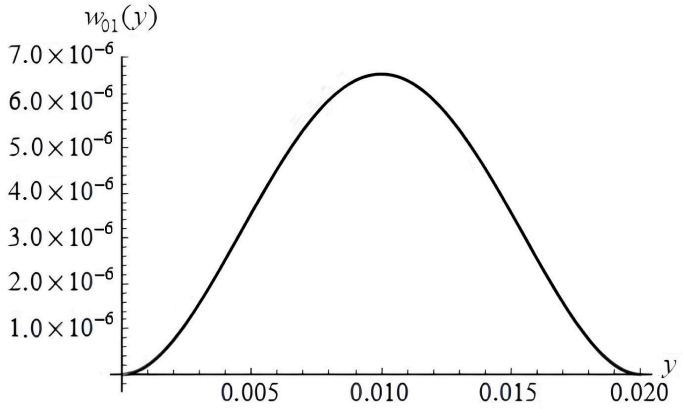

Figure 2. Initial approximation of plate deflection.

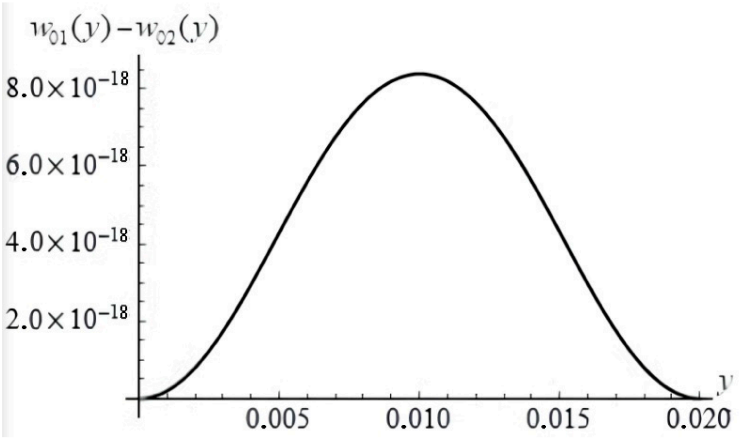

Figure 3. Initial effect of the longitudinal force nonlinearity.

As can be seen from Figure 3, the nonlinear longitudinal force resulting from the elongation of the plate due to its deformation leads to a decrease in the deflection of the plate.

5. Thermal Problem Solving

The solution to the thermal problem (17)–(22) is split into two parts: first the temperature distribution along the length of the pipe is found (Equations (17)–(19)), then the temperature distribution along the thickness of the plate (Equations (20)–(22)).

The solution to Equations (17)–(19) obtained through the separation of variables has the following form:

$$T_1(x,t) = T_*(t) - \sum_{n=0}^{\infty} \chi_n \cdot e^{-\gamma_n t} \sin \nu_n (x+l) \left[\frac{\beta^0 T_0}{\gamma_n} - T_1^0 + e^{\gamma_n t} \left(T_*(t) - \frac{\beta^0 T_0}{\gamma_n} \right) - a_1^2 \nu_n^2 \int_0^t e^{\gamma_n \tau} T_*(\tau) d\tau \right], \quad (32)$$

where $\gamma_n = a_1^2 \nu_n^2 + \beta^0$, $\nu_n = \frac{\pi(2n+1)}{2l}$, $\chi_n = \frac{4}{\pi(2n+1)}$, $T_1^0 = T_1(x,0) = const$, $a_1^2 = \frac{k_1}{\rho c_1}$, $\beta^0 = \frac{\beta}{\rho c_1}$.

Using Equation (32) it is possible to calculate the temperature at any point on the pipeline at any time t, if the law of temperature change $T_*(t)$ at the engine outlet is given.

The solution to Equations (20)–(22), which allows us to find the temperature distribution along the plate thickness at an arbitrary moment of time, has the following form:

$$T_2(x,t) = \widetilde{T}(t) + \sum_{n=0}^{\infty} A_n e^{-\delta_n t} \cos\mu_n(x-h)\left[T_2^0 - T_1^0 - \int_0^t e^{\delta_n t}\widetilde{T}'(t)dt\right] =$$
$$= \widetilde{T}(t) + \sum_{n=0}^{\infty} A_n e^{-\delta_n t} \cos\mu_n(x-h)\left[T_2^0 - T_1^0 - \sum_{k=0}^{\infty} \frac{\chi_k \cdot \gamma_k \sin\nu_k l}{\delta_n - \gamma_k}\left(\frac{\beta^0 T_0}{\gamma_k} - T_1^0 + \frac{a_1^2\nu_k^2 T_*}{\gamma_k}\right)\left(e^{(\delta_n-\gamma_k)t} - 1\right)\right], \quad (33)$$

where $T_2^0 = T_2(x,0) = const$, $a_2^2 = \frac{k_2}{\rho_0 c_2}$, $A_n = \frac{(-1)^n 2\alpha\sqrt{\alpha^2+\lambda_2^2\mu_n^2}}{\mu_n\left[h(\alpha^2+k_2^2\mu_n^2)+k_2\alpha\right]}$, $\delta_n = a_2^2\mu_n^2$, and the values μ_n $(n = 0 \div \infty)$ are the positive roots of the following equation:

$$\operatorname{tg}\mu_n h = \frac{\alpha}{k_2\mu_n}. \quad (34)$$

The function $\widetilde{T}(t) = T_1(0,t)$ is defined by Equation (32).

Substituting (33), we find the coefficient

$$N_1(t) = \frac{E\alpha_{T1}}{1-\nu}\int_0^h T_2(x,t)dx = \frac{E\alpha_{T1}}{1-\nu}\left(\widetilde{T}(t)h + \sum_{n=0}^{\infty}\frac{A_n}{\mu_n}e^{-\delta_n t}\sin\mu_n h\left[T_2^0 - T_1^0 - \int_0^t e^{\delta_n t}\widetilde{T}'(t)dt\right]\right) =$$
$$= \frac{E\alpha_{T1}}{1-\nu}\left(\widetilde{T}(t)h + \sum_{n=0}^{\infty}\frac{A_n}{\mu_n}e^{-\delta_n t}\sin\mu_n h\left[T_2^0 - T_1^0 - \sum_{k=0}^{\infty}\frac{\chi_k\cdot\gamma_k\sin\nu_k l}{\delta_n-\gamma_k}\left(\frac{\beta^0 T_0}{\gamma_k} - T_1^0 + \frac{a_1^2\nu_k^2 T_*}{\gamma_k}\right)\left(e^{(\delta_n-\gamma_k)t}-1\right)\right]\right). \quad (35)$$

Let the medium surrounding the pipeline be air with temperature $T_0 = 293.15$. The heat transfer coefficient between the surface of the pipeline and the environment is $\beta = 15.5$. Let us assume that the temperature at the inlet of the pipeline is constant $T_* = 1800$. The working medium in a pipeline of length $l = 0.5$ and width $H = 0.02$ is water, where density $\rho = 1000$, heat capacity coefficient $c_1 = 4182$, and heat transfer coefficient $k_1 = 0.683$. Assume that the plate thickness $h = 7 \times 10^{-4}$ is made of aluminium; then, the modulus of elasticity is $E = 7 \times 10^{10}$, Poisson's ratio is $\eta = 0.34$, thermal coefficient of linear expansion is $\alpha_T = 12.3 \times 10^{-6}$, heat capacity coefficient is $c_2 = 897$, and heat transfer coefficient is $k_2 = 209.3$. All values are given in the SI system.

Figure 4 shows the temperature variation along the length of the pipeline.

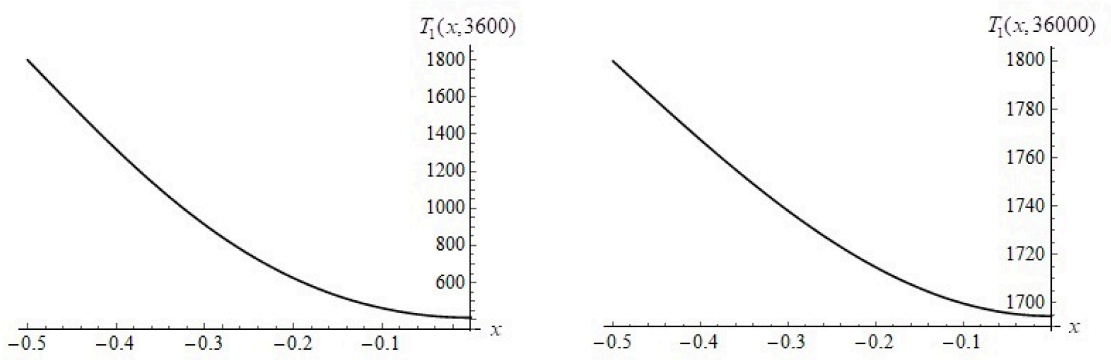

(**a**) (**b**)

Figure 4. Change in temperature of the working medium along the length of the pipeline: (**a**) at time points $t = 3600$; (**b**) at time points $t = 36{,}000$.

As can be seen from Figure 4, the temperature of the medium at the boundary with the plate (position $x = 0$) starts to increase with time.

Figure 5 shows the change in the temperature of the working medium at the plate boundary over time $t \in [0,\ 3600]$.

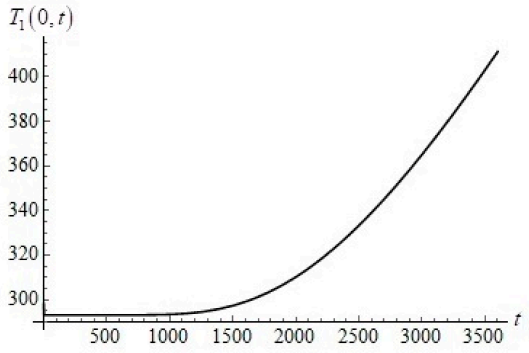

Figure 5. Temperature change in the working medium at the plate boundary.

Substituting the found function $\widetilde{T}(t) = T_1(0,t)$, shown in Figure 5, from (35) we obtain the function $N_1(t)$.

6. Solution of the Aerohydrodynamic Problem

Let us solve the aerohydrodynamic Equations (25), (26), (28) and (29). Assume that the overpressure does not depend on the coordinate y, i.e., $P_*(y,t) = P_*(t)$. Then, we will find the potential $\varphi(x,y,t)$ in the following form:

$$\varphi(x,y,t) = -\frac{1}{\rho}\int_0^t P_*(z)dz + (x+l)\alpha(t) + \sum_{n=1}^{\infty}\varphi_n(t)\cos\lambda_n y \cdot \mathrm{sh}\lambda_n(x+l), \qquad \lambda_n = \frac{n\pi}{H}. \tag{36}$$

Equation (36) satisfies the Laplace Equation (25), Equation (29) and the non-flow conditions on the pipeline walls $\varphi_y(x,0,t) = \varphi_y(x,H,t) = 0$. We will look for the function $w_1(y,t)$ in the form of a series expansion over the full system of functions $\{\xi_n(y)\}_{n=1}^{\infty}$ on the segment $[0,H]$, satisfying the boundary conditions corresponding to the conditions of rigid fixation of the plate ends (11).

According to (11), we will find the function $w_1(y,t)$ in the form

$$w_1(y,t) = \sum_{n=1}^{\infty} w_n(t)\xi_n(y), \tag{37}$$

where

$$\xi_n(y) = \mathrm{ch}(\mu_n y) - \cos(\mu_n y) - \frac{\mathrm{ch}(\mu_n H) - \cos(\mu_n H)}{\mathrm{sh}(\mu_n H) - \sin(\mu_n H)}(\mathrm{sh}(\mu_n y) - \sin(\mu_n y)), \tag{38}$$

and μ_n is obtained from the equation $\mathrm{ch}(\mu_n H)\cos(\mu_n H) = 1$.

Let us substitute (36), (37) into Equation (26).

$$\alpha(t) + \sum_{n=1}^{\infty}\varphi_n(t)\cos\lambda_n y \cdot \lambda_n \mathrm{ch}\lambda_n(w_0(y)+l) + \lambda_n w_{0y}(y)\sum_{n=1}^{\infty}\varphi_n(t)\sin\lambda_n y \cdot \mathrm{sh}\lambda_n(w_0(y)+l) = \sum_{n=1}^{\infty} w_{nt}(t)\xi_n(y), \tag{39}$$

According to the Galerkin method, we project (39) onto the complete system of functions $\{\cos\lambda_k y\}_{k=0}^{\infty}$. Projecting onto the first verification function $\cos\lambda_0 y = 1$, we obtain

$$\alpha(t)\cdot H + \sum_{n=1}^{\infty}\varphi_n(t)\lambda_n\int_0^H \left(\cos\lambda_n y \mathrm{ch}\lambda_n(w_0(y)+l) + w_{0y}(y)\sin\lambda_n y\,\mathrm{sh}\lambda_n(w_0(y)+l)\right)dy = \sum_{n=1}^{\infty} w_{nt}(t)\int_0^H \xi_n(y)dy.$$

Hence,

$$\alpha(t) = -\frac{1}{H}\sum_{n=1}^{\infty}\varphi_n(t)\lambda_n\int_0^H\left(\cos\lambda_n y\,\mathrm{ch}\lambda_n(w_0(y)+l) + w_{0y}(y)\sin\lambda_n y\,\mathrm{sh}\lambda_n(w_0(y)+l)\right)dy + \\ +\frac{1}{H}\sum_{n=1}^{\infty}w_{nt}(t)\int_0^H\xi_n(y)dy. \tag{40}$$

Let us introduce the notations

$$A_n = \lambda_n\int_0^H\left(\cos\lambda_n y\,\mathrm{ch}\lambda_n(w_0(y)+l) + w_{0y}(y)\sin\lambda_n y\ \ \mathrm{sh}\lambda_n(w_0(y)+l)\right)dy,\ B_n = \int_0^H\xi_n(y)dy. \tag{41}$$

Then, from (40) we obtain

$$\alpha(t) = -\frac{1}{H}\sum_{n=1}^{\infty}A_n\varphi_n(t) + \frac{1}{H}\sum_{n=1}^{\infty}B_n w_{nt}(t). \tag{42}$$

Projecting (39) onto the remaining functions $\{\cos\lambda_k y\}_{k=1}^{\infty}$, according to the Galerkin method, we obtain

$$\sum_{n=1}^{\infty}\varphi_n(t)\lambda_n\int_0^H\left(\cos\lambda_n y\,\mathrm{ch}\lambda_n(w_0(y)+l) + w_{0y}(y)\sin\lambda_n y\ \ \mathrm{sh}\lambda_n(w_0(y)+l)\right)\cos\lambda_k y dy + \\ +\alpha(t)\int_0^H\cos\lambda_k y dy = \sum_{n=1}^{\infty}w_{nt}(t)\int_0^H\xi_n(y)\cos\lambda_k y dy,\ \ k=1,2,\ldots \tag{43}$$

Let us introduce the notations

$$C_{nk} = \lambda_n\int_0^H\left(\cos\lambda_n y\,\mathrm{ch}\lambda_n(w_0(y)+l) + w_{0y}(y)\sin\lambda_n y\ \ \mathrm{sh}\lambda_n(w_0(y)+l)\right)\cos\lambda_k y dy,\ V_{nk} = \int_0^H\xi_n(y)\cos\lambda_k y dy. \tag{44}$$

Considering that

$$\int_0^H\cos\lambda_k y dy = 0, \tag{45}$$

from (43), we obtain

$$\sum_{n=1}^{\infty}V_{nk}w_{nt}(t) = \sum_{n=1}^{\infty}C_{nk}\varphi_n(t),\quad k=1,2,\ldots \tag{46}$$

Hence, from (46) we obtain a system of homogeneous equations

$$\sum_{n=1}^{\infty}\left(V_{nk}w_{nt}(t) - C_{nk}\varphi_n(t)\right) = 0,\quad k=1,2,\ldots \tag{47}$$

Let us substitute (36), (37) into Equation (28)

$$W_2\left(w_0(y), \sum_{n=1}^{\infty}w_n(t)\xi_n(y)\right) = P_*(t) - \rho(w_0(y)+l)\alpha_t(t) - \rho\sum_{n=1}^{\infty}\varphi_{nt}(t)\cos\lambda_n y\cdot\mathrm{sh}\lambda_n(w_0(y)+l). \tag{48}$$

Projecting (48) onto the system of functions $\{\xi_k(y)\}_{k=1}^{\infty}$, according to the Galerkin method, we obtain

$$\int_0^H W_2\left(w_0(y), \sum_{n=1}^{\infty}w_n(t)\xi_n(y)\right)\xi_k(y)dy = P_*(t)\cdot\int_0^H\xi_k(y)dy - \rho\alpha_t(t)\int_0^H(w_0(y)+l)\xi_k(y)dy - \\ -\rho\sum_{n=1}^{\infty}\varphi_{nt}(t)\int_0^H\cos\lambda_n y\cdot\mathrm{sh}\lambda_n(w_0(y)+l)\cdot\xi_k(y)dy\,,\quad k=1,2,\ldots \tag{49}$$

Let us introduce the notations

$$D_k = \rho \int_0^H (w_0(y) + l)\xi_k(y)dy,\ E_{nk} = \rho \int_0^H \cos\lambda_n y \cdot \mathrm{sh}\lambda_n(w_0(y) + l) \cdot \xi_k(y)dy. \quad (50)$$

Then, substituting (42), from (49) we obtain

$$\int_0^H W_2\left(w_0(y), \sum_{n=1}^{\infty} w_n(t)\xi_n(y)\right)\xi_k(y)dy = B_k P_*(t) + \frac{D_k}{H}\sum_{n=1}^{\infty} A_n\varphi_{nt}(t) - \frac{D_k}{H}\sum_{n=1}^{\infty} B_n w_{ntt}(t) - \sum_{n=1}^{\infty} E_{nk}\varphi_{nt}(t)\ ,\ \ k = 1, 2, \ldots \quad (51)$$

As a result, we obtain a system of ordinary differential Equations (47) and (51) for determining the unknown functions $\varphi_n(t)$, $w_n(t)$.

7. Numerical Experiment

Let us perform a numerical experiment for models (8) and (9), limiting the number of summands in expansions (36) and (37) to m.

Let the medium surrounding the pipeline be air with temperature $T_0 = 293.15$. The heat transfer coefficient between the surface of the pipeline and the environment $\beta = 15.5$. Let us assume that the temperature at the inlet of the pipeline is constant $T_* = 1800$, and the overpressure is variable $P_*(t) = 10^6(5 - \cos 10t)$. The working medium in a pipeline of length $l = 0.5$ and width $H = 0.02$ is water; then, the density $\rho = 1000$, heat capacity coefficient $c_1 = 4182$, and heat conductivity coefficient $k_1 = 0.683$. Let the difference between the pressure in the resting medium and the external load distributed on the plate be $P_0 - \overline{P} = 2 \times 10^4$. Suppose that the plate thickness $h = 7 \times 10^{-4}$ is made of aluminium; then, density $\rho_0 = 2700$, modulus of elasticity $E = 7 \times 10^{10}$, Poisson's ratio $\eta = 0.34$, thermal coefficient of linear expansion $\alpha_T = 12.3 \times 10^{-6}$, heat capacity coefficient $c_2 = 897$, thermal conductivity coefficient $k_2 = 209.3$, bending stiffness $D = \frac{Eh^3}{12(1-\nu^2)} = 2262$, and linear mass $M = \rho_0 h = 1.89$. Assume that the constant component of force $N_0 = 10^5$, the stiffness coefficient of the crimped plate layer $\gamma = 4$, and the other coefficients are as follows: $\mu = 30$, $\eta = 10$, $\beta_1 = 4$, $\beta_2 = 4$. All values are given in the SI system.

Let us take the initial conditions $T_1^0 = 293.15$, $T_2^0 = 293.15$, $w_k(0) = 0$, $w_{kt}(0) = 0$, $k = 1, \ldots, m$.

Solving the system (47), (51) in Mathematica 12.0, taking the segments of series in the formulas of length $m = 8$, we construct the graphs of the deformation function $w(y,t) = w_0(y) + \varepsilon\sum_{n=1}^{m} w_n(t)\xi_n(y)$.

Consider the linear model of a deformable solid (8). Substituting $L_2\left(w_0(y), \sum_{n=1}^{m} w_n(t)\xi_n(y)\right)$ into (51), we obtain

$$\begin{aligned}\int_0^H \Bigg(M\sum_{n=1}^{\infty} w_{ntt}(t)\xi_n(y) + D\sum_{n=1}^{\infty} w_n(t)\xi_{nyyyy}(y)\ + N_1(t)w_{0yy} + N_0\sum_{n=1}^{\infty} w_n(t)\xi_{nyy}(y) + \gamma\sum_{n=1}^{\infty} w_n(t)\xi_n(y) + \\ +\beta_1\sum_{n=1}^{m} w_{nt}(t)\xi_n(y) + \beta_2\sum_{n=1}^{m} w_{nt}(t)\xi_{nyyyy}(y)\Bigg)\xi_k(y)dy = B_k P_*(t) + \frac{D_k}{H}\sum_{n=1}^{\infty} A_n\varphi_{nt}(t) - \\ -\frac{D_k}{H}\sum_{n=1}^{\infty} B_n w_{ntt}(t) - \sum_{n=1}^{\infty} E_{nk}\varphi_{nt}(t)\ ,\ \ k = 1, 2, \ldots\end{aligned} \quad (52)$$

Let us introduce the notations

$$F_{nk} = \int_0^H \xi_{nyyyy}(y)\xi_k(y)dy,\ J_k = \int_0^H w_{0yy}\xi_k(y)dy,\ G_{nk} = \int_0^H \xi_{nyy}(y)\xi_k(y)dy. \quad (53)$$

https://doi.org/10.3390/engproc2026150129

Given (41) and the orthogonality of the functions (38) on the segment $[0, H]$:

$$\int_0^H \xi_n(y)\xi_k(y)dy = 0, \quad n \neq k, \quad \int_0^H \xi_k^2(y)dy = H, \tag{54}$$

we obtain

$$\sum_{n=1}^{\infty}\left[\left(MH\delta_{nk} + \frac{D_k B_n}{H}\right)w_{ntt}(t) + (\beta_1 H\delta_{nk} + \beta_2 F_{nk})w_{nt}(t) + (DF_{nk} + N_0 G_{nk} + \gamma H\delta_{nk})w_n(t) - \right.$$
$$\left. - \left(\frac{D_k A_n}{H} - E_{nk}\right)\varphi_{nt}(t)\right] = B_k P_*(t) - J_k N_1(t), \quad k = 1, 2, \ldots \tag{55}$$

Figure 6 shows the deformations of the plate at time $t = 5$ (Figure 6a) and $t = 20$ (Figure 6b) at $m = 8$. Figure 7 shows the deformations of the plate at the midpoint $y = 0.01$ of the plate at $t \in [0, 5]$ (Figure 7a) and $t \in [0, 20]$ (Figure 7b) at $m = 8$.

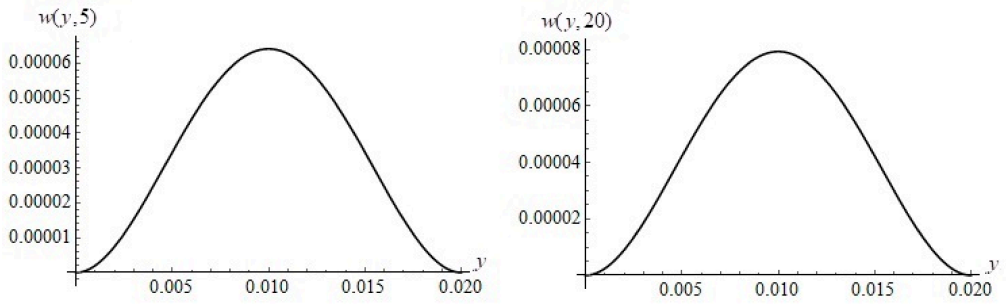

(**a**) (**b**)

Figure 6. Deformation of the plate at times $t = 5$ (**a**) and $t = 20$ (**b**) for $m = 8$.

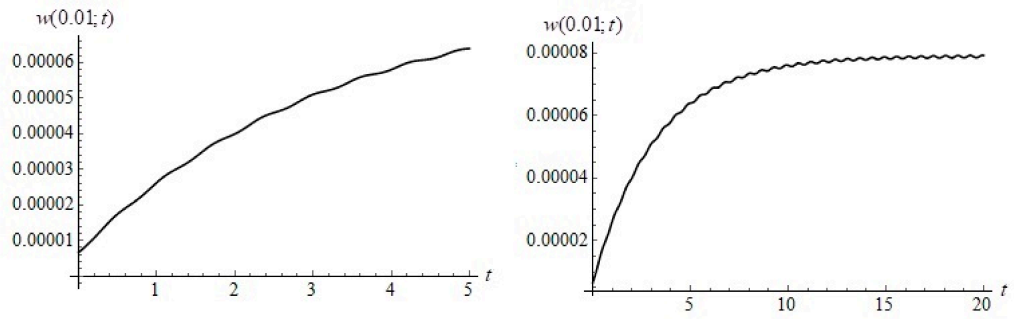

(**a**) (**b**)

Figure 7. Deformation of the plate at the point $y = 0.01$, $t \in [0, 5]$ (**a**) and $t \in [0, 20]$ (**b**), $m = 8$.

Let us consider the nonlinear model of a deformable solid (9). Substituting $J_2\left(w_0(y), \sum_{n=1}^{m} w_n(t)\xi_n(y)\right)$ into (51), we obtain

$$\int_0^H \left(M\sum_{n=1}^{m} w_{ntt}(t)\xi_n(y) + D\sum_{n=1}^{m} w_n(t)\xi_{nyyyy}(y) + N_1(t)w_{0yy} + N_0\sum_{n=1}^{m} w_n(t)\xi_{ny}(y) + \gamma\sum_{n=1}^{m} w_n(t)\xi_n(y) + \right.$$
$$+\beta_1\sum_{n=1}^{m} w_{nt}(t)\xi_n(y) + \beta_2\sum_{n=1}^{m} w_{nt}(t)\xi_{nyyyy}(y) - \mu\sum_{n=1}^{m} w_n(t)\xi_{nyy}(y)\int_0^H w_{0y}^2(y)dy -$$
$$\left. -2w_{0yy}\left(\mu\sum_{n=1}^{m} w_n(t)\int_0^H w_{0y}(y)\xi_{ny}(y)dy + \eta\sum_{n=1}^{m} w_{nt}(t)\int_0^H w_{0y}(y)\xi_{ny}(y)dy\right)\right)\xi_k(y)dy =$$
$$= B_k P_*(t) + \frac{D_k}{H}\sum_{n=1}^{m} A_n\varphi_{nt}(t) - \frac{D_k}{H}\sum_{n=1}^{m} B_n w_{ntt}(t) - \sum_{n=1}^{m} E_{nk}\varphi_{nt}(t), \quad k = 1, 2, \ldots \tag{56}$$

Let us introduce the notations

$$U = \int_0^H w_{0y}^2(y)dy,\ Q_k = \int_0^H w_{0y}\xi_{ky}(y)dy. \tag{57}$$

Then, taking into account (41), (53), and (54), we obtain

$$\sum_{n=1}^{\infty}\left[\left(MH\delta_{nk} + \frac{D_kB_n}{H}\right)w_{ntt}(t) + (\beta_1 H\delta_{nk} + \beta_2 F_{nk} - 2\eta Q_n J_k)w_{nt}(t) + (DF_{nk} + N_0 G_{nk} + \gamma H\delta_{nk} - \right.$$
$$\left. -\mu U G_{nk} - 2\mu Q_n J_k)w_n(t) - \left(\frac{D_k A_n}{H} - E_{nk}\right)\varphi_{nt}(t)\right] = B_k P_*(t) - J_k N_1(t),\ \ k = 1,2,\ldots \tag{58}$$

Figure 8 shows the calculations for $m = 8$ at $t = 5$ (Figure 8a) and $t = 20$ (Figure 8b), where $w_{lin}(y,t),\ w_{non}(y,t)$ are the plate deformations obtained by solving the system of Equations (55) and (58), respectively.

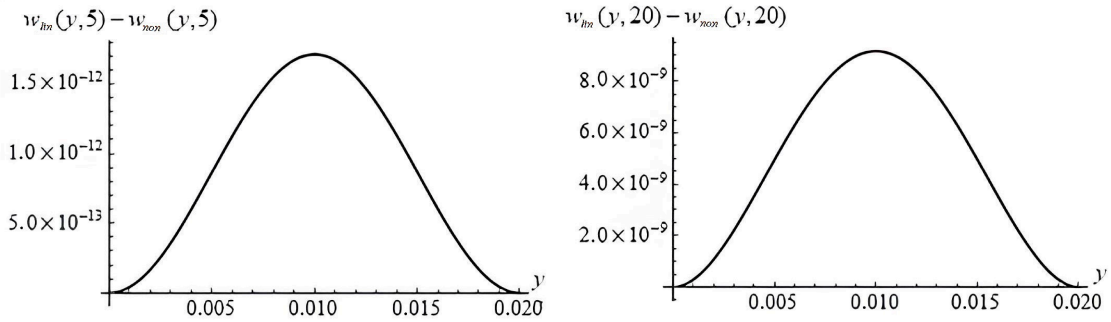

(**a**) (**b**)

Figure 8. The difference in the plate deformation in models (8) and (9) at times $t = 5$ (**a**) and $t = 20$ (**b**) for $m = 8$.

Figure 8 shows the difference between the solutions of the linear and nonlinear models. As we can see from Figure 8, the effect of nonlinearity of the longitudinal force has an insignificant effect on the magnitude of the plate deflection, while the plate deflection decreases.

8. Conclusions

The paper studies the joint dynamics of the pressure sensor and the working medium in the pipeline on the basis of linear and nonlinear mathematical models that take into account the initial deformation of the elastic element and the transfer of heat flow through the pipeline with the working medium from the motor to the elastic element. The study of the elastic element dynamics is based on the application of the small parameter method, Galerkin method and numerical experiment in Mathematica 12.0. The case of rigid fixation of the elastic element ends is considered. The above approach can also be applied to pipelines with modified end geometry. A comparative analysis of the results obtained for the linear and nonlinear model is carried out.

Author Contributions: Conceptualization, P.V. and A.A.; methodology, P.V.; software, A.A.; formal analysis, P.V. and A.A.; investigation, P.V. and A.A.; data curation, P.V. and A.A.; writing—original draft preparation, A.A.; writing—review and editing, P.V.; visualisation, P.V. and A.A.; supervision, P.V. and A.A.; project administration, P.V.; funding acquisition, P.V. All authors have read and agreed to the published version of the manuscript.

Funding: The work was supported by a grant from the Russian Science Foundation No. 23-21-00517.

Institutional Review Board Statement: Not applicable.

Informed Consent Statement: Informed consent was obtained from all subjects involved in the study.

Data Availability Statement: The raw data supporting the conclusions of this article will be made available by the authors on request.

Conflicts of Interest: The authors declare no conflicts of interest.

References

1. Chehreghani, M.; Misra, A.K.; Paidoussis, M.P. Dynamics of a cantilevered pipe conveying fluid and partially subjected to a confined counter-current external axial flow of a different fluid. *J. Sound Vib.* **2024**, *590*, 118574. [CrossRef]
2. Shaaban, A.; Chehreghani, M.; Misra, A.K.; Paidoussis, M.P. Experiments on the dynamics of aspirating cantilevered pipes concurrently subjected to reverse external axial flow. *J. Sound Vib.* **2023**, *561*, 117817. [CrossRef]
3. Aulisa, E.; Ibragimov, A.; Kaya-Cekin, E.Y. Fluid structure interaction problem with changing thickness beam and slightly compressible fluid. *Discret. Contin. Dyn. Syst.* **2014**, *7*, 1133–1148. [CrossRef]
4. Faal, R.T.; Derakhshan, D. Flow-Induced Vibration of Pipeline on Elastic Support. *Procedia Eng.* **2011**, *14*, 2986–2993. [CrossRef]
5. Kheiri, M.; Paidoussis, M.P. Dynamics and stability of a flexible pinned-free cylinder in axial flow. *J. Fluids Struct.* **2015**, *55*, 204–217. [CrossRef]
6. Giacobbi, D.B.; Semler, C.; Paidoussis, M.P. Dynamics of pipes conveying fluid of axially varying density. *J. Sound Vib.* **2020**, *473*, 115202. [CrossRef]
7. Abdelbaki, A.R.; Paidoussis, M.P.; Misra, A.K. A nonlinear model for a hanging cantilevered pipe discharging fluid with a partially-confined external flow. *Int. J. Non-Linear Mech.* **2020**, *118*, 103290. [CrossRef]
8. Mogilevich, L.I.; Popova, E.V. Longitudinal waves in the walls of an annular channel filled with liquid and made of a material with fractional nonlinearity. *Izv. Vyss. Uchebnykh Zaved. Prikl. Nelineynaya Din.* **2023**, *31*, 365–376.
9. Blinkov, Y.A.; Blinkova, A.Y.; Evdokimova, E.V.; Mogilevich, L.I. Mathematical modeling of nonlinear waves in an elastic cylindrical shell surrounded by an elastic medium and containing a viscous incompressible liquid. *Acoust. Phys.* **2018**, *64*, 274–279. [CrossRef]
10. Mogilevich, L.I.; Popov, V.S.; Popova, A.A.; Christoforova, A.V.; Popova, E.V. Mathematical modeling of three-layer beam hydroelastic oscillations. *Vibroeng. Procedia* **2017**, *12*, 12–18. [CrossRef]
11. Mogilevich, L.I.; Popov, V.S.; Popova, A.A. Longitudinal and transverse oscillations of an elastically fixed wall of a wedge-shaped channel installed on a vibrating foundation. *J. Mach. Manuf. Reliab.* **2018**, *47*, 227–234. [CrossRef]
12. Velmisov, P.A.; Ankilov, A.V.; Semenova, E.P. Mathematical modeling of aeroelastic systems. In *Applications of Mathematics in Engineering and Economics (AMEE'17)*; Pasheva, V., Popivanov, N., Venkov, G., Eds.; AIP Conference Proceedings 1910; AIP Publishing LLC: Melville, NY, USA, 2017; pp. 1–8. [CrossRef]
13. Velmisov, P.A.; Ankilov, A.V.; Pokladova, Y.V. Stability of solutions of initial-boundary value problems in aerohydroelasticity. In *Applications of Mathematics in Engineering and Economics (AMEE'18)*; Pasheva, V., Popivanov, N., Venkov, G., Eds.; AIP Conference Proceedings 2048; AIP Publishing LLC: Melville, NY, USA, 2018; pp. 1–10. [CrossRef]
14. Velmisov, P.A.; Ankilov, A.V. Mathematical modeling of some aerohydroelastic systems. In *Applications of Mathematics in Engineering and Economics (AMEE'21)*; AIP Conference Proceedings 2371; AIP Publishing LLC: Melville, NY, USA, 2021; p. 040009.
15. Velmisov, P.A.; Pokladova, Y.V. Mathematical modelling of the "pipeline–pressure sensor" system. *J. Phys. Conf. Ser.* **2019**, *1353*, 012085. [CrossRef]
16. Velmisov, P.A.; Tamarova, Y.A.; Pokladova, Y.V. Mathematical modelling of pressure monitoring systems in fluid and gaseous media. In *Applications of Mathematics in Engineering and Economics (AMEE'20)*; AIP Conference Proceedings 2333; AIP Publishing LLC: Melville, NY, USA, 2021; p. 120004. [CrossRef]
17. Mihajlov, P.G.; Mokrov, E.A.; Mitrohin, S.V.; Sergeev, D.A. Features of metrological support for modern pressure pulsation sensors. *News South. Fed. Univ. Tech. Sci.* **2012**, *130*, 174–179. (In Russian)
18. Mikhailov, P.G.; Mokrov, E.A.; Sergeev, D.A.; Skotnikov, V.V.; Petrin, V.A.; Chernetsov, M.A. Sensitive elements of high-temperature pressure sensors. Materials and manufacturing technologies. *Izv. SFedU. Eng. Sci.* **2014**, *153*, 204–213. (In Russian)
19. Pirogov, S.P. *Manometric Tubular Springs*; Nedra: St. Petersburg, Russia, 2009. (In Russian)
20. Pirogov, S.P.; Cherentsov, D.A.; Chuba, A.Y.; Ustinov, N.N. Simulation of forced oscillations of pressure monitoring devices. *Int. J. Eng. Trends Technol.* **2022**, *70*, 32–36. [CrossRef]
21. Etkin, L.G. *Vibration Frequency Sensors. Theory and Practice*; Publishing house of MSTU N.E. Bauman: Moscow, Russia, 2004. (In Russian)
22. Belozubov, E.M.; Vasiliev, V.A.; Zapevalin, A.I.; Chernov, P.S. Design of elastic components of nano- and microelectromechanical systems. *Meas. Tech.* **2011**, *54*, 21–24. [CrossRef]
23. Dmitrienko, A.G.; Isakov, S.A.; Belozubov, E.M. Pressure sensors based on nano- and microelectromechanical systems for rocket and aviation technology. *Sens. Syst.* **2012**, *160*, 19–25. (In Russian)

24. Belozubov, E.M.; Mokrov, E.A.; Tikhomirov, D.V. Minimizing the error of thin-film strain-resistive pressure sensors under the influence of non-stationary temperature. *Sens. Syst.* **2004**, *1*, 26–29. (In Russian)
25. Stuchebnikov, V.; Vaskov, Y.; Savchenko, E. Special pressure sensors of the MIDA industrial group. *Compon. Technol.* **2021**, *238*, 12–15. (In Russian)
26. Kazaryan, A.A.; Groshev, G.P. Universal pressure transducer. *Meas. Tech.* **2008**, *51*, 269–275. [CrossRef]
27. Savchenko, E.G.; Stuchebnikov, V.M.; Ustinov, A.A. Features of the design of high-temperature strain gauge pressure transducers based on SNS structures. *Instruments* **2016**, *189*, 1–7. (In Russian)

Disclaimer/Publisher's Note: The statements, opinions and data contained in all publications are solely those of the individual author(s) and contributor(s) and not of MDPI and/or the editor(s). MDPI and/or the editor(s) disclaim responsibility for any injury to people or property resulting from any ideas, methods, instructions or products referred to in the content.